Novel Mechanism for Interesting C−C Coupling and Cleavage Reactions and Control of Thermodynamic Stability Involving [L₂M(μ-CCR)₂ML₂] and [L₂M(μ-RCC-CCR)ML₂] Complexes (M = Ti, Zr; L = η^5-C₅H₅, Cl, H; R = H, F, CN): A Theoretical Study[1]

Eluvathingal D. Jemmis* and Kalathingal T. Giju

Contribution from the School of Chemistry, University of Hyderabad, Central University P.O., Hyderabad-500 046, India

Received August 5, 1997

Abstract: Possible reaction mechanisms for C−C coupling and cleavage reactions involving [(η^5-C₅H₅)M-(μ-CCR)₂M(η^5-C₅H₅)₂] and [(η^5-C₅H₅)M(μ-RCC-CCR)M(η^5-C₅H₅)₂] (M = Ti, Zr) complexes are discussed on the basis of theoretical studies. A series of realistic and simplified model complexes, [L₂M(μ-CCR)₂ML₂] **8** and [L₂M(μ-RCC-CCR)ML₂] **9** (M = Ti, Zr; L = η^5-C₅H₅, Cl, H; R = H, F, CN) were calculated using ab initio MO and density functional methods. The formation of the bisacetylide bridging complex starting from either metal acetylides or butadiyne is explained by a mechanistic scheme involving metallacyclocumulenes (**5**), binuclear complexed metallacyclocumulenes (**6**), and the M⁺²−M⁺⁴ complexes (**7**). The latter rather than **6** led to the C−C coupled products **9** via **8**. The experimentally observed unusual C−C coupling in the dimeric bis(η^5-cyclopentadienyl)phenylethynyltitanium complex and the lack of it in the corresponding zirconium complex are influenced by substituents on the ethynyl group. Theoretical studies demonstrate that the electron-withdrawing substituent R = F drives the thermodynamic equilibrium distinctively towards the C−C coupled product, **9** both for M = Ti and Zr. An unusually short Zr−Zr interatomic distance in [(η^5-C₅H₅)Zr(μ-CCR)₂-Zr(η^5-C₅H₅)₂] compared to Ti−Ti distance in the corresponding Ti complex is observed theoretically and from X-ray crystal structures of related complexes. Substitution of cyclopentadienyls by Cl and even H to obtain computationally viable models does not change the relative energies of the ground and transition states of the binuclear Zr complexes. The Ti complexes are affected somewhat more by these changes but the trends in relative energies between Ti and Zr isomers are retained. Geometric parameters and relative energies obtained at the B3LYP/LANL2DZ level are found to be better than those at the HF level.

Introduction

Biscyclopentadienyltitanium (Cp₂Ti) and biscyclopentadienylzirconium (Cp₂Zr) and their derivatives form ubiquitous fragments in early transition metal organometallic chemistry.[2] Several industrially important catalytic reactions are based on these fragments.[3] Often dramatic contrasts exist in the reactivity of Ti and Zr complexes. One of them triggered our interest in this study. Almost three decades ago Teuben and de Liefde Meijer suggested structures **1a** or **2a** (Scheme 1) for the dimer of bis(η^5-cyclopentadienyl)phenylethynyltitanium that they had synthesized.[4] An X-ray structure analysis by Sekutowski and

Stucky in 1976 of a related compound, [(η^5-C₅H₄CH₃)₂Ti(μ-PhC₄Ph)Ti(η^5-C₅H₄CH₃)₂] showed it to have a C−C coupled geometry **3b**; this as well as spectral data demonstrated that Teuben's compound also has a similar C−C coupled structure, (**3a**).[5] In addition, it was shown that **3b** can be obtained starting from Ph−C≡C−C≡C−Ph. Dedicated efforts of several researchers over the years established the delicate balance that exists between the structures **2** and **3** for Ti as a function of the substituents on the bridging acetylides or butadiynes.[6−10] Naturally, curiosity in the C−C coupling and cleaving reactions mediated by Ti led to reactions involving Zr.[8,11−15] Early on Erker and co-workers showed by X-ray crystallography that the

(1) Presented in part at the 9th International Congress of Quantum Chemistry, Emory University, Atlanta, Georgia, June 9−14, 1997. Taken in part from the Ph.D. thesis of K.T.G., University of Hyderabad, 1997.

(2) (a) Lauher, J. W.; Hoffmann, R. *J. Am. Chem. Soc.* **1976,** *98,* 1729. (b) Bochmann, M. in *Comprehensive Organometallic Chemistry II*; Abel, E. W., Stone, F. G. A., Wilkinson, G., Eds.; Pergamon Press: New York, 1997; Vol. 4, Chapters 4 and 5. (c) Negishi, E.; Takahashi, T. *Acc. Chem. Res.* **1994,** *27,* 124. (d) Doherty, S.; Corrigan, J. F.; Carty, A. J.; Sappa, E. *Adv. Organomet. Chem.* **1995,** *37,* 39. (e) Lotz, S.; Rooyen, P. H. V.; Meyer, R. *Adv. Organomet. Chem.* **1995,** *37,* 219. (f) Lancaster, S. J.; Robinson, O. B.; Bochmann, M.; Coles, S. J.; Hursthouse, M. B. *Organometallics* **1995,** *14,* 2456.

(3) (a) Crabtree, R. H. *The Organometallic Chemistry of the Transition Metals*; John Wiley: New York, 1994. (b) Bottrill, M.; Gavens, P. D.; Kelland, J. W.; McMeeking, J. In *Comprehensive Organometallic Chemistry*; Wilkinson, G., Stone, F. G. A., Abel, E. W., Eds.; Pergamon Press: New York, 1982; Vol. 3, Chapter 22.5.

(4) Teuben, J. H.; de Liefde Meijer, H. J. *J. Organomet. Chem.* **1969,** *17,* 87.

(5) Sekutowski, D. G.; Stucky, G. D. *J. Am. Chem. Soc.* **1976,** *98,* 1376.

(6) Wood, G. L.; Knobler, C. B.; Hawthorne, M. F. *Inorg. Chem.* **1989,** *28,* 382.

(7) Rosenthal, U.; Görls, H. *J. Organomet. Chem.* **1992,** *439,* C36.

(8) Cuenca, T.; Gómez, R.; Gómez-Sal, P.; Rodriguez, G. M.; Royo, P. *Organometallics* **1992,** *11,* 1229.
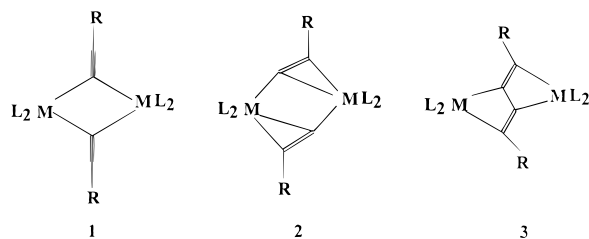
(9) Rosenthal, U.; Ohff, A.; Tillack, A.; Baumann, W.; Görls, H. *J. Organomet. Chem.* **1994,** *468,* C4.

(10) Varga, V.; Mach, K.; Hiller, J.; Thewalt, U.; Sedmera, P.; Polasek, M. *Organometallics* **1995,** *14,* 1410.

(11) (a) Erker, G.; Frömberg, W.; Mynott, R.; Gabor, B.; Krüger, C. *Angew. Chem., Int. Ed. Engl.* **1986,** *25,* 463. (b) Erker, G. *Angew. Chem., Int. Ed. Engl.* **1989,** *28,* 397. (c) Erker, G.; Frömberg, W.; Benn, R.; Mynott, R.; Angermund, D.; Kruger, C. *Organometallics* **1989,** *8,* 911.

(12) Metzler, N.; Nöth, H. *J. Organomet. Chem.* **1993,** *454,* C5.

C–C Coupling and Cleavage Reactions

J. Am. Chem. Soc., Vol. 120, No. 28, 1998 6953

Scheme 1. Experimentally Reported Structures of Various Symmetrical Homobinuclear Titanium and Zirconium Complexes Which Formed the Basis of the Present Investigation

	L_2	M	R	1	2	3	ref.
a	Cp_2	Ti	Ph			3	4
b	$(C_5H_4Me)_2$	Ti	Ph			3	5
c	Cp_2	Ti	$SiMe_3$		2		6,7
d	$(C_5H_4)_2SiMe_2$	Ti	Ph	1	2	3	8
e	Cp_2	Ti	CMe_3			3	9
f	$(C_5H_3Me_2)_2$	Ti	$SnMe_3$		2		10
g	$Cp(\mu\text{-}\eta^5\text{-}C_5H_4\text{-})$	Zr	Ph		2		8
h	$(C_5H_4Me)_2$	Zr	Ph		2		11
i	Cp_2	Zr	$SiMe_3$		2		12,16
j	$Cp(\mu\text{-}\eta^5\text{-}C_5H_4\text{-})$	Zr	$SiMe_3$		2		13
k	$(\eta^5\text{-}C_5H_4\text{-})(\eta^5\text{-}C_5H_3\text{-}SiMe_3)SiMe_2$	Zr	$SiMe_3$		2		14
l	Cp_2	Zr	^nBu		2		15

binuclear Zr complex with bridging alkynyl ligands has the structure **2h**.[11a] In fact, detailed studies showed that the structure is fluxional, but in no case was the Zr complex with the C–C coupled product **3h** isolated.[11c] A change of ligands to the bridged cyclopentadienyls also did not yield the complex of structure **3**; only $[(\eta^5\text{-}Cp)Zr(\mu\text{-}C\equiv CPh)]_2(\mu\text{-}\eta^5\text{-}\eta^5C_{10}H_8)$ (**2g**) was isolated.[8] Metzler and Nöth tried the trimethylsilylacetylides as starting ligands but Zr complexes did not proceed beyond **2i**.[12] Buchwald and co-workers observed that butadiyne led to C–C cleaved product with Cp_2Zr reagent.[16] However this contrast is not universal. Rosenthal et al. studied these systems extensively in an effort to suggest a suitable reaction mechanism, which can be summarized in Scheme 2.[17,18] According to this, the in situ generated starting material Cp_2M reacts with buta-1,3-diyne to give a metallacyclocumulene **5**. This is also generated from the isomerization of the bisacetylide complex **4**. The middle C–C bond of the cumulene unit in **5** binds to another Cp_2M fragment to give **6**. This binuclear complex is not isolated but is considered to be a connecting point for different products such as **2**, **3**, and **7**.[17] This mechanistic proposal was based on structures of other homo- or heterobinuclear transition metal complexes isolated previously.[18] Except for the formation of **3**, all other reactions in this scheme are observed for both Ti and Zr complexes. Thus it is clear that

the chemistry of Ti and Zr provides many similarities along with dramatic contrasts. Similarly Lang et al. proposed possible intermediate steps (Scheme 3) in forming uncoupled Zr complex **2**.[14] This included a paramagnetic complex of type **1** which was also suggested by Royo et al. even though there is no conclusive structural evidence.[8,13] If these reactions are indeed reversible, there exists a possibility for alkane metathesis (eq 1).[19] According to Rosenthal, if the butadiyne can give

$$R\text{–}C\equiv C\text{–}C\equiv C\text{–}R +$$
$$R'\text{–}C\equiv C\text{–}C\equiv C\text{–}R' \rightarrow 2R\text{–}C\equiv C\text{–}C\equiv C\text{–}R' \quad (1)$$

bisacetylide complex, and if there is an exchange of acetylides possible at some stage of the reaction, it is possible to get a different butadiyne than what is started with.[19] This has now been observed experimentally.[19c]

There is no comprehensive theoretical study attempted to delineate these mechanistic details so far. An early MO study based on extended Hückel theory suggested closed-shell species corresponding to **2** and **3**, but could not explain the absence of C–C coupling in the Zr complexes.[20] In a preliminary report, substituent effect on thermodynamic preference for **2** and **3** was presented.[21] On the basis of the analysis of various reactions and previous suggestions we have formulated Scheme 4 which accommodates most of the experimental observations. This forms the beginning point of the present theoretical examination.

Comparison of the X-ray crystal structure data of similar Ti and Zr complexes **2** (Scheme 1) shows that the Zr–Zr distance is shorter compared to the Ti–Ti distance, i.e., 3.522 Å (**2i**) and 3.550 Å (**2c**), respectively. This is interesting for the following reasons. Conventional electron counting leads to +3 oxidation state and d^1 electron count for the metals in **2**. The covalent radius of Zr is larger than that of Ti. Despite this the Zr–Zr distance is shorter than that of the Ti–Ti distance. Previously the contrasting M–M distance in similar complexes of paramagnetic $Cr_2Cl_9^{3-}$ ion[22] and diamagnetic $W_2Cl_9^{3-}$ ion[23] were attributed to the absence of metal–metal bond in the former and the presence of it in the latter.[24] But in **2** both Ti and Zr complexes are diamagnetic and the M–M distances are considerably longer than standard metal–metal bond lengths. It was explained that the diamagnetism observed for these M(III) complexes of **2** is due to either an antiferromagnetic coupling[6] or an electronic coupling.[19] However, the shorter M–M distance in Zr complex has remained without explanation. Recently a diamagnetic binuclear Ti(III) complex with bridging formamidinate complex has been reported.[25] The Ti–Ti distance of 2.942 Å observed experimentally and the HOMO that indicates direct M–M and through bridge interactions account for the diamagnetism of this complex. The Ti–Ti and Zr–Zr distances in **2** are much longer. The origin of diamagnetism in these complexes is an open question. In this paper we study these and different mechanistic steps outlined in Scheme 4 using ab initio MO and density functional methods. In addition, the contrasting behavior of Ti and Zr chemistry

(13) Cano, A.; Cuenca, T.; Galakhov, M.; Rodríguez, G. M.; Royo, P.; Cardin, C. J.; Convery, M. A. *J. Organomet. Chem.* **1995**, *493*, 17.

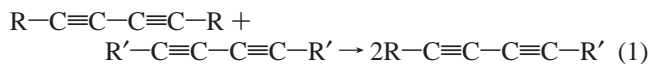(14) Lang, H.; Blau, S.; Nuber, B.; Zsolnai, L. *Organometallics* **1995**, *14*, 3216.

(15) Heshmatpour, F.; Wocadlo, S.; Massa, W.; Dehnicke, K. *Acta Crystallogr.* **1995**, *C51*, 2225.

(16) Hsu, D. P.; Davis, W. M.; Buchwald, S. L. *J. Am. Chem. Soc.* **1993**, *115*, 10394.

(17) Pulst, S.; Arndt, P.; Heller, B.; Baumann, W.; Kempe, R.; Rosenthal, U. *Angew. Chem., Int. Ed. Engl.* **1996**, *35*, 1112.

(18) (a) Ohff, A.; Pulst, C.; Lefeber, C.; Peulecke, N.; Arndt, P.; Burlakov, V. V.; Rosenthal, U. *Synlett* **1996**, 111. (b) Pellny, P.-M.; Peulecke, N.; Burlakov, V. V.; Tillack, A.; Baumann, W.; Spannenberg, A.; Kempe, R.; Rosenthal, U. *Angew. Chem., Int. Ed. Engl.* **1997**, *36*, 2615.

(19) (a) Rosenthal, U.; Ohff, A.; Baumann, W.; Kempe, R.; Tillack, A.; Burlakov, V. V. *Organometallics* **1994**, *13*, 2903. (b) Rosenthal, U.; Pulst, S.; Ohff, A.; Tillack, A.; Baumann, W.; Kempe, R.; Burlakov, V. V. *Organometallics* **1995**, *14*, 2961. (c) Pulst, S.; Kirchbauer, F. G.; Heller, B.; Baumann, W.; Rosenthal, U. *Angew. Chem.* **1998**, *110*, 2029.

(20) Pavankumar, P. N. V.; Jemmis, E. D. *J. Am. Chem. Soc.* **1988**, *110*, 125.

(21) Jemmis, E. D.; Giju, K. T. *Angew. Chem., Int. Ed. Engl.* **1997**, *36*, 606.

(22) Wessel, G. J.; Ijdo, D. J. W. *Acta Crystallogr.* **1957**, *10*, 466.

(23) Watson, W. H., Jr.; Waser, J. *Acta Crystallogr.* **1958**, *11*, 689.

(24) Cotton, F. A. *Rev. Pure Appl. Chem.* **1967**, *17*, 25.

(25) Hao, S.; Feghali, K.; Gambarotta, S. *Inor. Chem.* **1997**, *36*, 1745.

Scheme 2. Mechanistic Scheme Proposed by Rosenthal and Co-workers for Various Observed Complexes of Ti and Zr Acetylides[17,18]
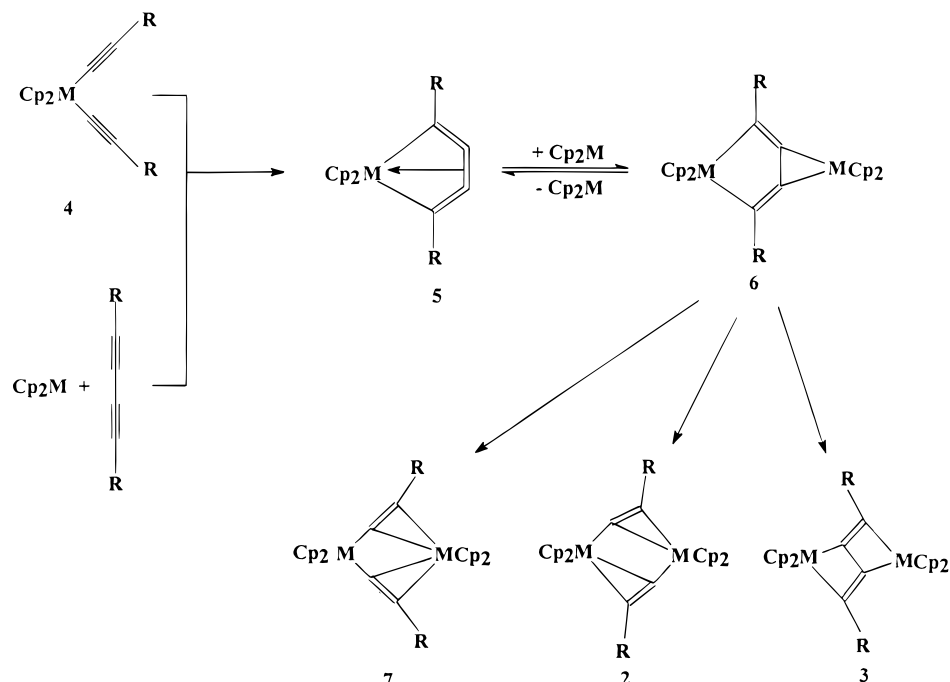
Scheme 3. Reaction Steps Proposed by Lang et al. for the Formation of Complex **2**[14]
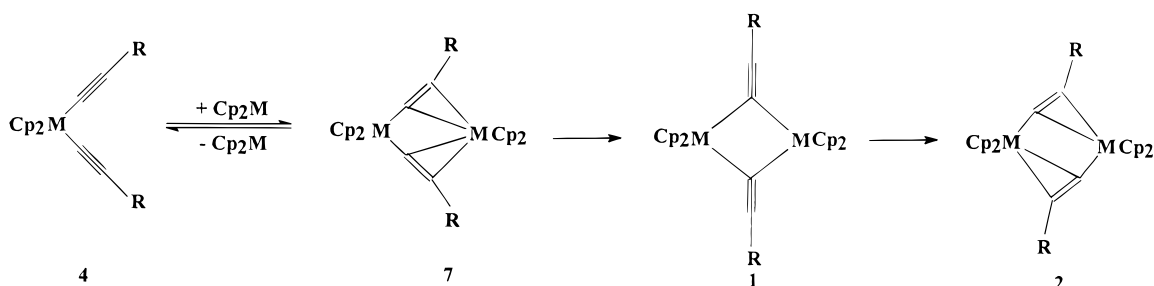
represented in Scheme 5 is discussed. These are important in view of the continuing interest in these C−C bond-forming reactions.[26]

In view of the large number of structures involved in this study, a uniform labeling that specifies the metals and substituents in the structures is necessary to keep the thread of discussion in tact. The transition metals involved are either Ti or Zr. The ligands L attached to them can be H, Cl, or Cp. The third variable is the substituent R on the acetylide or butadiyne. The R group is kept as H in most of the complexes, but the effect of substituents is probed by using CN and F in place of H. To take into account of all of these variables, the following labeling scheme is used (Scheme 5). A given number indicates a particular type of structure. The six metal−ligand combinations ML are indicated by the letters **a**−**f** that follow the number (Scheme 5). The next variable R is represented by a second letter added after the number: **a** for H, **b** for CN, and **c** for F. Thus in Scheme 5, **8db** indicates the following: **8d** corresponds to structure **8** with M = Zr and L = H. The next letter, **b**, indicates R = CN. A similar procedure is used in numbering the transition states. All transition structures are labeled as T followed by the number of the structures that are connected by the transition structure. This is followed by the
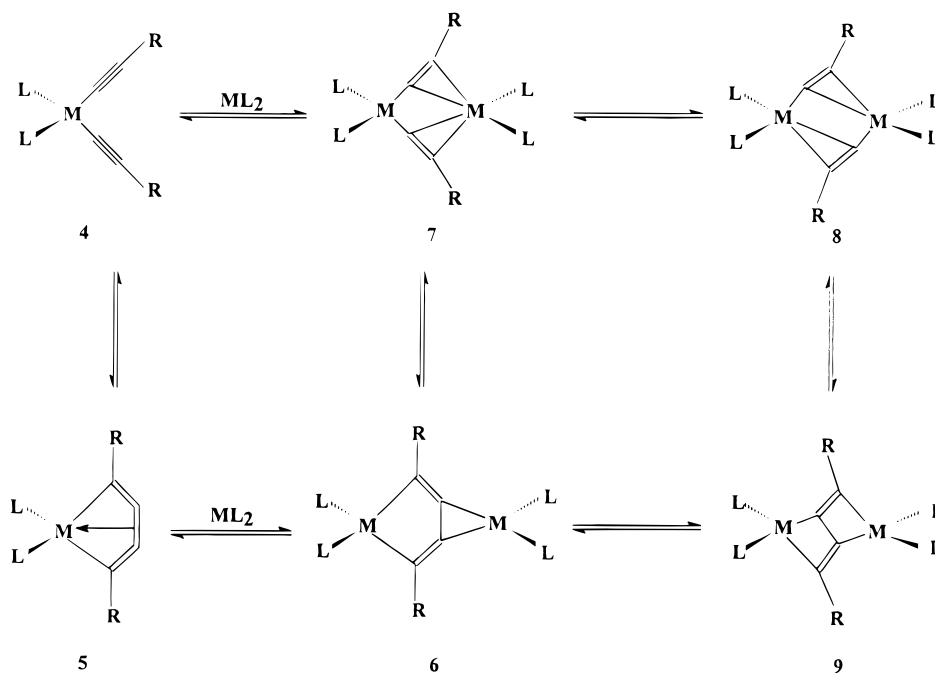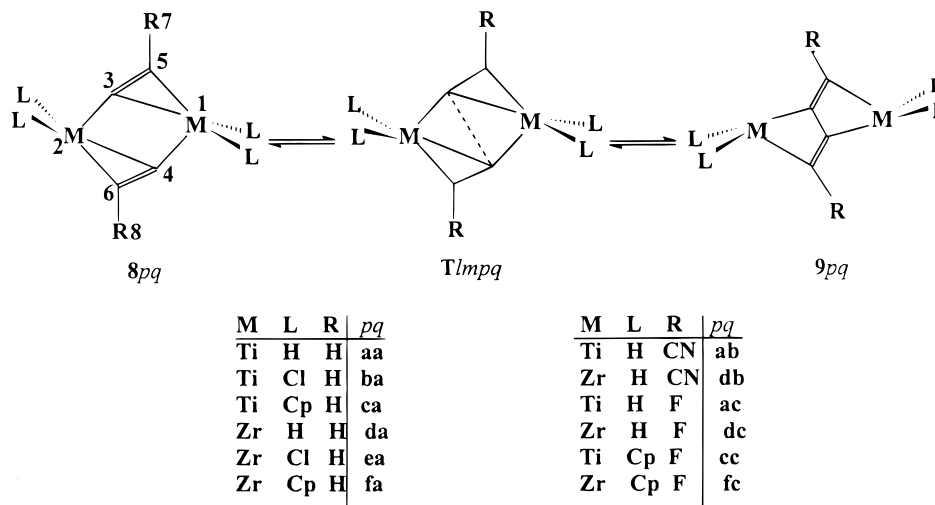
two letters which have the same significance as above. Thus **T89db** corresponds to a transition structure connecting **8** and **9** for M = Zr, L = H (from **d**) and R = CN (from **b**). Thus all structures discussed in the text can be understood by this convention.

Theoretical Methods and Selection of Models

For a study of this magnitude it was necessary to select practical models and theoretical methods that are appropriate. Several steps were taken to arrive at realistic models. There has been attempts to model cyclopentadienyl groups by Cl and H.[27] It was shown that Cl is a good replacement for Cp in transition metal organometallic chemistry, since such a replacement does not affect the essential electronic features of the system under consideration. We have followed a stepwise procedure to arrive at a model that is practical and at the same time realistic. In the first stage the substituted cyclopentadienyls were replaced by Cp. The substituents on acetylides and butadiynes were replaced by H. These structures (L = Cp and

(26) (a) Manna, J.; John, K. D.; Hopkins, M. D. *Adv. Organomet. Chem.* **1995**, *38*, 79. (b) Roettinger, D.; Erker, G.; Froehlich, R. *Chem. Ber.* **1995**, *128*, 1045.

(27) (a) Koga, N.; Morokuma, K. *Chem. Rev.* **1991**, *91*, 823 and references therein. (b) Radius, U.; Silverio, S. J.; Hoffmann, R.; Gleiter, R. *Organometallics* **1996**, *15*, 3737 and references therein.

Scheme 4. Suggested Mechanism for C−C Coupling Reactions Involving Ti and Zr Complexes

**Scheme 5.** Model Complexes **8** and **9** Chosen for **2** and **3** Respectively[a]

M	L	R	pq
Ti	H	H	aa
Ti	Cl	H	ba
Ti	Cp	H	ca
Zr	H	H	da
Zr	Cl	H	ea
Zr	Cp	H	fa

M	L	R	pq
Ti	H	CN	ab
Zr	H	CN	db
Ti	H	F	ac
Zr	H	F	dc
Ti	Cp	F	cc
Zr	Cp	F	fc

[a] *p* stands for combination of M and L ranging from **a** to **f**. *q* stands for R and ranges from **a** to **c**. *l* and *m* are numerics corresponding to the number of structures connected by the transition structure.

R = H) were optimized at the B3LYP level[28] using the pseudopotential basis given below. The relative energies of the structural pairs **8ca** and **9ca**, and **8fa** and **9fa** showed that the C−C coupled product is favorable for Ti, but the bisacetylide structure is preferred for Zr (Figure 1). This is in accord with the experimental results discussed above. Following the previous theoretical observations that Cl can effectively be used as a model for Cp, the relative energies are calculated by replacing every cyclopentadienyl by Cl (**8,9 ba**, **ea**; Figure 1). The C−C coupled structure at this stage is unfavorable for both Ti and Zr, but the relative energetics between Ti and Zr vis-à-vis **8** and **9** is retained. For a detailed study of the mechanistic details, even these systems are too large. Thus while several calcula-

tions were carried out with this model, further simplification was sought by replacing the Cl by H. As Figure 1 indicates, this did not change the energetics substantially. For this reason most calculations were carried out using these two models. For a limited set of molecules, calculations were carried out with L = Cp under C_{2h} symmetry constraints for fully optimized geometry. The range of molecules required in this study restricted our choice of methods to HF or B3LYP for obvious reasons. Relative energies calculated at these two levels using the effective core potentials (ECP) of Hay and Wadt[29] along with the valence basis sets, available in Gaussian94 package[30] as LANL2DZ indicated that the differences were not very large. Besides, the experimental observation of uniformly shorter Zr−Zr distances than Ti−Ti distances in **2** is reproduced at the B3LYP level only. For these reasons the B3LYP level, which

(28) B3LYP is Becke's three parameter hybrid method using the LYP correlation functional. (a) Becke, A. D. *J. Chem. Phys.* **1993**, *98,* 5648. (b) Lee, C.; Yang, W.; Parr, R. G. *Phys. Rev. B* **1988**, *37*, 785. (c) Vosoko, S. H.; Wilk, L.; Nusair, M. *Can. J. Phys.* **1980**, *58*, 1200. (d) Stephens, P. J.; Delvin, F. J.; Chabalowski, C. F.; Frisch, M. J. *J. Phys. Chem.* **1994**, *98*, 11623.

(29) (a) Hay, P. J.; Wadt, W. R. *J. Chem. Phys.* **1985**, *82*, 270. (b) Wadt, W. R.; Hay, P. J. *J. Chem. Phys.* **1985**, *82*, 284. (c) Hay, P. J.; Wadt, W. R. *J. Chem. Phys.* **1985,** *82*, 299.
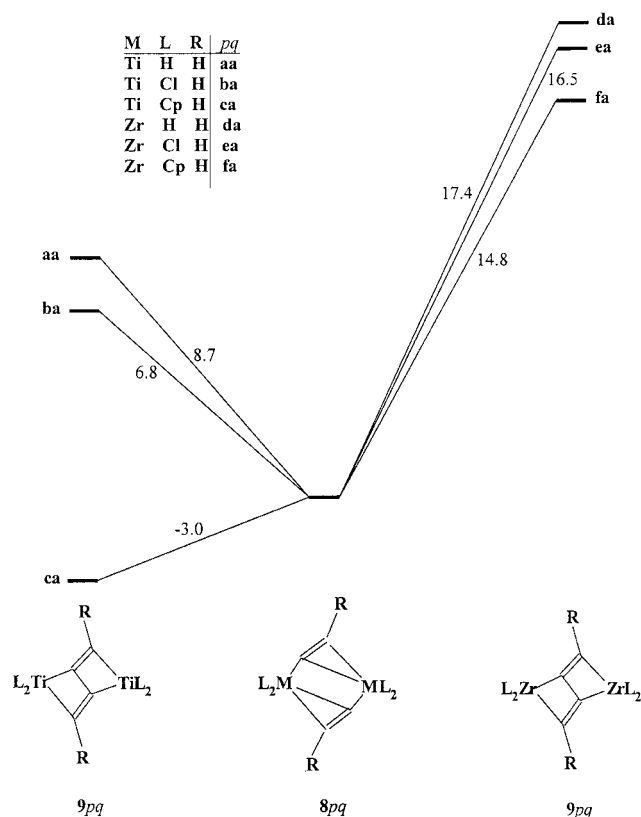
Figure 1. Comparison of relative energies (kcal/mol) at the B3LYP level of the complexes **8** and **9** with M = Ti, Zr, L = H, Cl, Cp, and R = H. Structures of **8** are kept at the reference value of 0.0.

is by far the most economical way of including electron correlation, is selected as the method of choice. Thus all calculations were carried out at the B3LYP level using LANL2DZ for all atoms. On optimization, structure **8cc** collapsed into **9cc**. Transition structures connecting the minima of binuclear complexes are also calculated at the same level of theory except for the structures with L = Cp. These were located using an eigenvalue following optimization method.[31] Numerical vibrational frequency calculations were performed on the model structures (L = H, Cl) to ascertain the nature of the stationary point. The total energies, zero point vibrational energies, and thermal correction to Gibbs free energy along with coordinates of all the species studied in this paper are given in the Supporting Information. Important geometric parameters for complexes with L = Cp are given in Table 1 and those for the other **8** and **9** structures along with the corresponding transition structures are summarized in Table 2. Table 3 gives natural charges and Wiberg bond indices[32] based on natural bond orbital analysis (NBO).[33] The geometric parameters of the

(30) Frisch, M. J.; Trucks, G. W.; Schlegel, H. B.; Gill, P. M. W.; Johnson, B. G.; Robb, M. A.; Cheeseman, J. R.; Keith, T.; Petersson, G. A.; Montgomery, J. A.; Raghavachari, K.; Al-Laham, M. A.; Zakrzewski, V. G.; Ortiz, J. V.; Foresman, J. B.; Cioslowski, J.; Stefanov, B. B.; Nanayakkara, A.; Challacombe, M.; Peng, C. Y.; Ayala, P. Y.; Chen, W.; Wong, M. W.; Andres, J. L.; Replogle, E. S.; Gomperts, R.; Martin, R. L.; Fox, D. J.; Binkley, J. S.; Defrees, D. J.; Baker, J.; Stewart, J. P.; Head-Gordon, M.; Gonzalez, C.; Pople, J. A. *Gaussian 94, Revision D.2*; Gaussian, Inc.: Pittsburgh, PA, 1995.
(31) (a) Baker, J. *J. Comput. Chem.* **1986**, *7*, 385. (b) Baker, J. *J. Comput. Chem.* **1987**, *8*, 563.
(32) (a) Wiberg, K. B. *Tetrahedron* **1968**, *24*, 1083. (b) Mayer, I. *Theor. Chim. Acta* **1985**, *67*, 315.
(33) (a) Reed, A. E.; Weinstock, R. B.; Weinhold, F. *J. Chem. Phys.* **1985**, *83*, 735. (b) Reed, A. E.; Weinhold, F. *J. Chem. Phys.* **1985**, *83*, 1736. (c) Reed, A. E.; Weinhold, F.; Curtiss, L. A. *Chem. Rev.* **1988**, *88*, 899.

intermediates and the transition structures of the mechanistic scheme are given in Figures 2 and 3. Figures 5 and 6 give the potential energy surfaces (PESs) for the reaction mechanisms of Scheme 6. The potential energy surfaces for the isomerization of **8** → **9** is given in Figure 7. The energetics of the mechanistic scheme is discussed first. A part of the scheme involving **8** and **9** which shows maximum difference between Ti and Zr is discussed next. This is followed by a general discussion of the charges calculated from the natural electron population analysis.

Results and Discussion

(a) Reaction Mechanism. The plausible mechanisms for the reactions leading to the structures **2** and **3** from the reactive metallocene, Cp_2M, have been investigated using the models indicated in Scheme 6. Figures 2 and 3 give geometries and natural charges of various intermediates (**4**−**9**). The model for the reactive fragment, ML_2, reacts with butadiyne to give a bisacetylide complex (**4**) or metallacyclocumulene (**5**). The metallacyclocumulene is thermodynamically more stable than the bisacetylide complex. This result is interesting because the highly strained structure **5** would normally have been thought as less stable. The metal−carbon and carbon−carbon distances obtained for these models are comparable to those found experimentally for the complexes.[11c,34,35] The experimental observation of the photochemical conversion of the metallacyclocumulene to the bisacetylide complex supports the calculated relative energies. Although both these complexes have their metals in the formal +4 oxidation state, the thermodynamic stability of **5** over **4** could be explained satisfactorily from the additional π-coordination of the middle π-bond of cumulene. The bisacetylide complex **4** reacts again with one molecule of ML_2 in a highly exothermic process to form redox complex **7** with one metal center formally in the +4 and the other in +2 oxidation states. On the other hand, in a similar but somewhat less exothermic process complex **5** gives **6**. The longer middle C−C bond distance in the C_4 unit of the latter justifies the description of C_4 as a buta-1,3-diene tetraanion making both metals formally +4. Thermodynamically **7** is favored over **6** partly because of the absence of stabilization due to π-coordination toward the metal center in the latter complexes. The frontier molecular orbitals of **5** and **6** indicate that the new metal−π interactions do not have optimum orbital hybridizations for best overlap even though **6** is a minimum (Figure 4). It appears that **6** can also rearrange to **9** by the inversion of one C≡C bond. This has been suggested as a possible step in the mechanism (Scheme 2). This is also calculated to be thermodynamically favorable for Ti and Zr. However the M−M axes in **6** are orthogonal to the middle C−C bonds which are already highly stretched for a conjugated carbon chain, making its activation more feasible. For example, the interaction of the in-plane π*-orbitals of H−C≡C−C≡C−H with the metal d levels (Figure 4c) has largely increased this bond on going from **5** to **6** (Figures 2 and 3). In another isomerization step, **7** is converted to **8**. The relative energy difference between **7** and **8** is ∼1 kcal mol^{-1}. It is easy to see that the movements of atoms needed to take **8** to **9** is not very large. These studies indicate that the thermodynamic preferences of ground-state structures are not sufficient for deciding mechanistic steps. The

(34) Burlakov, V. V.; Ohff, A.; Lefeber, C.; Tillack, A.; Baumann, W.; Kempe, R.; Rosenthal, U. *Chem. Ber.* **1995**, *128*, 967.
(35) Rosenthal, U.; Ohff, A.; Baumann, W.; Kempe, R.; Tillack, A.; Burlakov, V. V. *Angew. Chem., Int. Ed. Engl.* **1994**, *33*, 1605.

Scheme 6. Reaction Energies (kcal/mol) between Various Minima on the Potential Energy Surface of Mechanistic Steps for Ti and Zr Acetylide Complexes at the B3LYP Level Including ZPE Corrections[a]


	M	L	R
aa	Ti	H	H
ba	Ti	Cl	H
da	Zr	H	H
ea	Zr	Cl	H
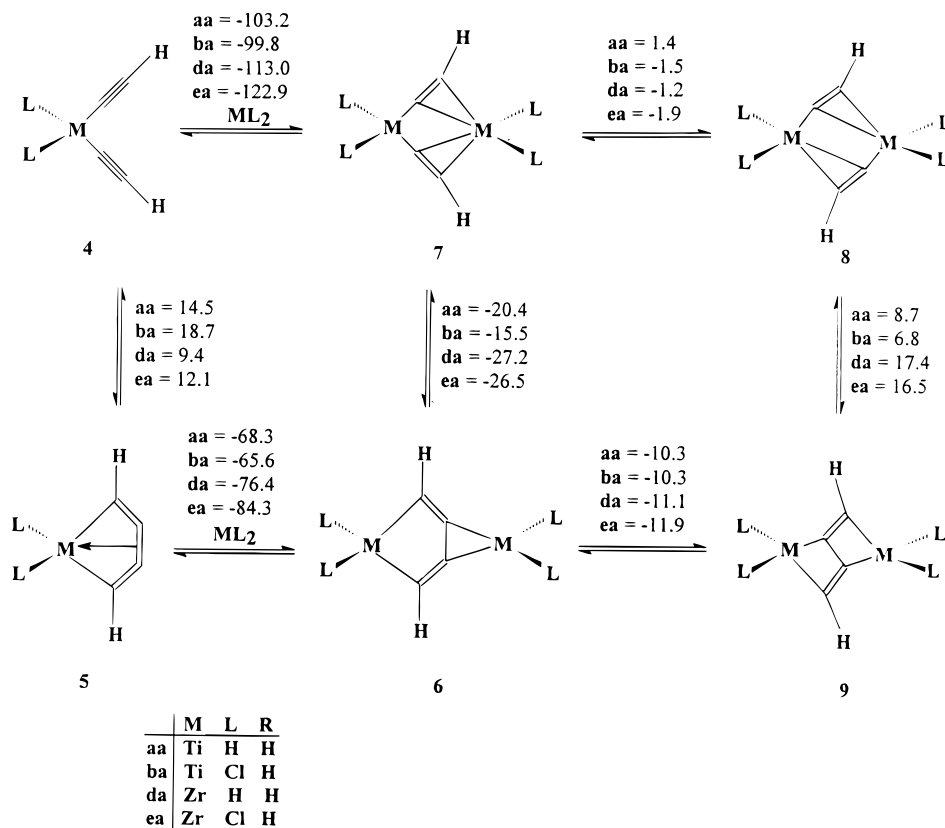
[a] All ML$_2$ fragments are calculated in their singlet states. The singlet structure for ZrCl$_2$ is not a minimum at this level.

reaction barriers have to be taken into account. For this purpose we have carried out calculations for transition structures involved in most of these individual transformations. The geometries and natural charges on atoms are given in Figures 2 and 3.

The potential energy diagram for the overall reaction mechanism including various transition structures are shown in the Figure 5 for Ti complexes and in the Figure 6 for Zr complexes. Comparison of barriers helps to predict favorable pathways. The conversion of the cumulene complex **6** to **9** suggested in the experimental Scheme 4 is calculated to have the highest barrier (∼34.0 kcal/mol) on the PES. The same conversion can be effected through **7** and **8**. The barriers for the isomerization reaction **6** → **7** via **T67** are calculated to be practically nil (∼0.0 kcal/mol). The next steps **7** → **8** also have reasonably low barrier heights of 10.5−14.5 kcal/mol (**T78**), justifying the dynamic processes observed in solution. Our calculations on the triplet states of **1** ([H$_2$M(CCH)$_2$MH$_2$], M = Ti, Zr), following the Scheme 3, indicate that these are mostly not minima and very much higher in energy than **T78aa** and **T78da**. Hence the involvement of **1**, as an intermediate or transition structure for isomerization of **7** to **8**, is most unlikely in the present reaction despite the existence of many complexes of other transition metals with similar structures. However, it is to be mentioned that reason for the observed paramagnetic behavior initially in the reaction remained inconclusive and Royo et al. attributed it to either the M^{+3} monomer or a symmetrically bridging dimer (**1**).[8,13] The final step involving the C−C bond formation **8** → **9** has barriers, 8.6−10.4 kcal/mol for Ti complexes and 17.2−18.1 kcal/mol for Zr complexes, respectively. This is the largest difference calculated between Ti and Zr in this set of reactions. Thus the analysis of different

mechanistic pathways outlined in Scheme 6 suggests the possibility of the reaction to proceed via **5**−**6**−**7**−**8**−**9** rather than any other pathways. Details of the transition structures give hints about the reason for high or low barriers. An interesting case in point is the transformations of **6** to **9** and **7** to **8** (Figures 2 and 3). Both involve shifting of a π-bonded C$_2$ unit from one metal to another. Yet the first transformation has a very high barrier compared to the second one. This is because the middle C−C bond of the C$_4$H$_2$ unit in **6** does not allow much room for adjustment in **T69** while **T78** has enough feasibility to retain reasonable geometry around the metal even in the transition structure. Among these the major step in distinguishing Ti from Zr in C−C coupling is **8** → **9**. Hence it is analyzed in greater detail below.

(b) Geometry of 2 and B3LYP vs HF. Despite the larger size of Zr, geometrical comparison of available X-ray structures of similar Ti and Zr complexes **2** (Table 1) show that the Zr−Zr distance is shorter compared to Ti−Ti distance (3.522 Å (**2i**) and 3.550 Å (**2c**), respectively). Although it was suggested that either an antiferromagnetic coupling or an electronic coupling could be the reasons for diamagnetism for these M(III) complexes, nothing is known about the shortening of M−M distance in Zr complex. We have calculated the geometries of complexes **8ca** and **8fa** at the HF and B3LYP levels (Table 1). Calculations at the HF level does not differentiate the M−M distances. On the other hand calculations at the B3LYP level reproduces the experimental observation that Zr−Zr distance is shorter than Ti−Ti distance in the corresponding complexes of **2**. However, a direct comparison of experimental and theoretical geometries is not possible considering the substituents present in the experimental systems and the effects in the crystal compared to a gas-phase calculation.
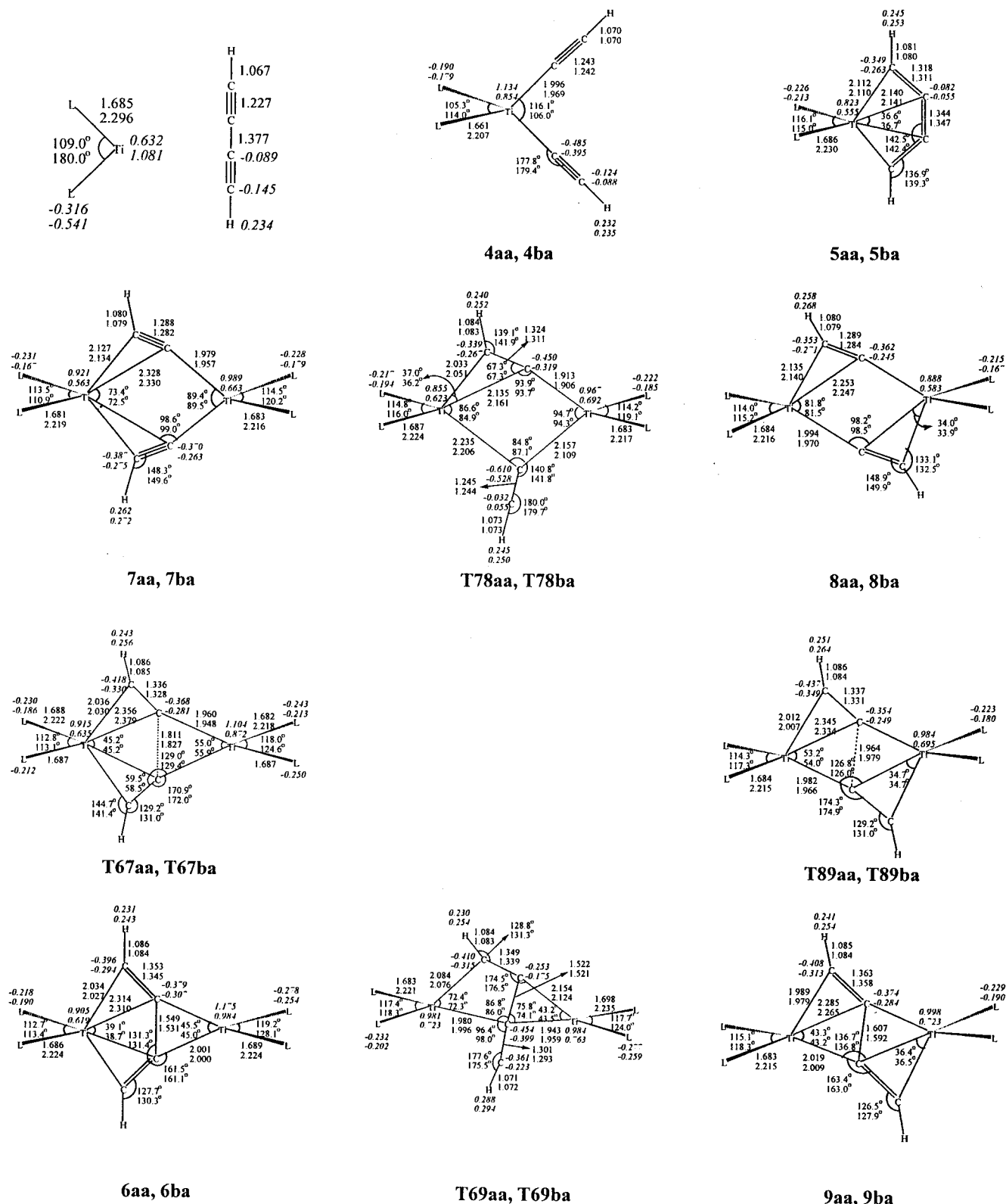
Figure 2. Geometries and natural charges (*italics*) on atoms of intermediates and transition structures for the reaction mechanism (Scheme 6) for Ti complexes at the B3LYP level. Bond lengths are in angstroms, and bond angles in degrees. The upper numbers of the pair corresponds to L = H (**aa**) and the lower numbers to L = Cl (**ba**). The imaginary frequencies for the transition structures are 355i (**T67aa**), 95i (**T78aa**), 269i (**T89aa**), 614i (**T69aa**), 366i (**T67ba**), 112i (**T78ba**), 255i (**T89ba**), and 546i (**T69ba**).

(c) The C–C Coupling and Decoupling (8 vs 9). The anomalous feature of the shorter Zr–Zr distance in comparison to Ti–Ti distance and the relevance of the step **8 → 9** in the reaction mechanism prompted us to investigate its role in the C–C coupling reaction. As discussed in the Introduction, Zr

complexes of the type **3** are not known. Relative energies (Figure 1) for Scheme 5 show that the Ti complexes **8ca** and **9ca** have almost same energy while the Zr complex **8fa** is considerably more favorable than **9fa**. These are in tune with the experiments. The complexes of the type **8ca**, **9ca**, and **8fa**
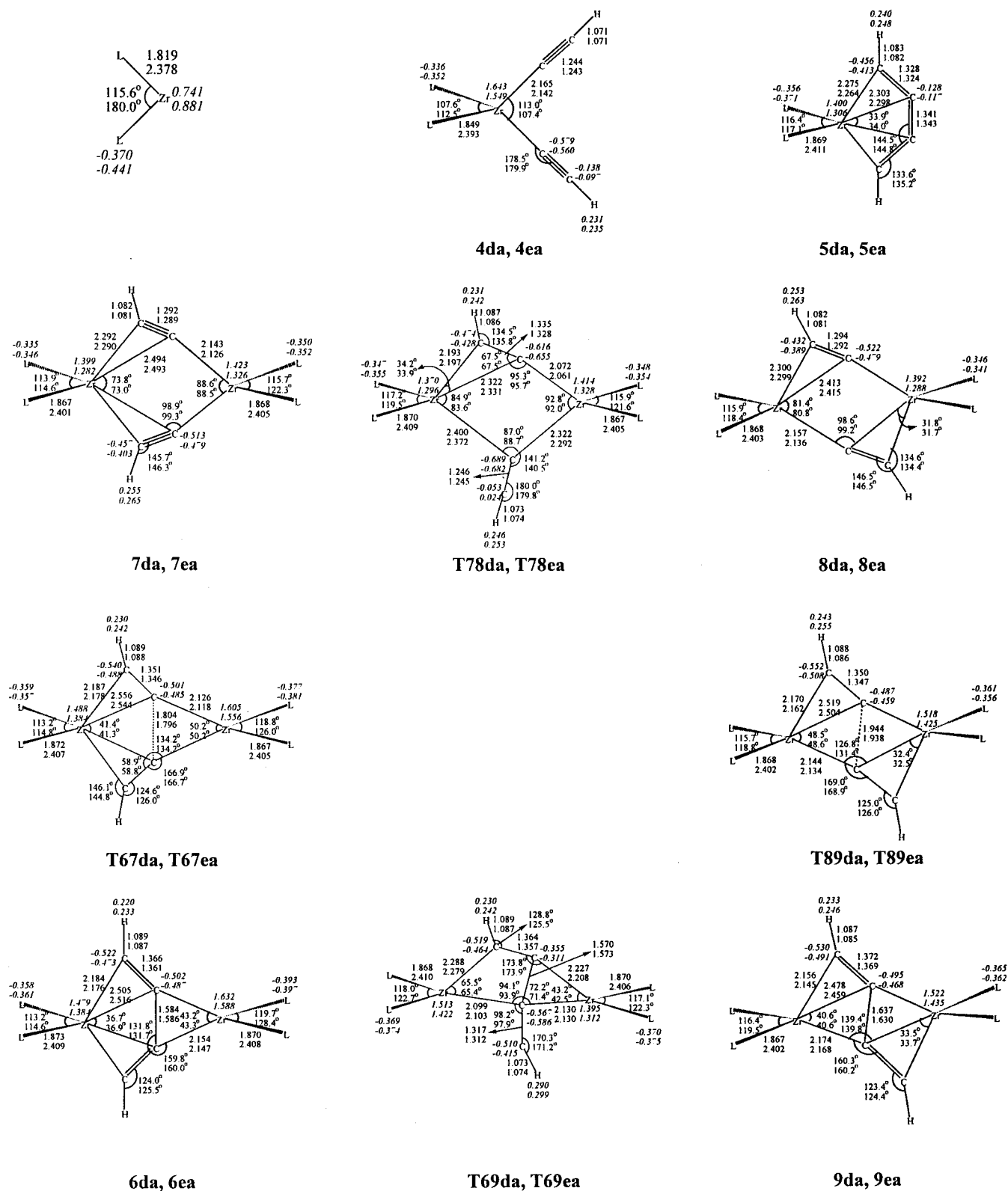
Figure 3. Geometries and natural charges (*italics*) on atoms of intermediates and transition structures for the reaction mechanism (Scheme 6) for Zr complexes at the B3LYP level. Bond lengths are in angstroms and bond angles in degrees. The upper numbers of the pair corresponds to L = H (**da**) and the lower numbers to L = Cl (**ea**). The imaginary frequencies for the transition structures are 327i (**T67da**), 140i (**T78da**), 257i (**T89da**), 643i (**T69da**), 324i (**T67ea**), 149i (**T78ea**), 255i (**T89ea**), and 593i (**T69ea**).

were isolated while examples of **9fa** are yet to be observed. The energetic balance between the Ti complexes **8ca** and **9ca** can be shifted one way or the other by varying the substituents and ligands. Experimentally a change from the phenyl substituent on the alkyne to Si(CH₃)₃ led to the preferential formation of the bisacetylide structure **2c** instead of the C−C

coupled product **3b** (Scheme 1).[6] The formation of the C−C cleaved product from (CH₃)₃Si−C≡C−C≡C−Si(CH₃)₃ dramatically demonstrates the ability of the binuclear template to reduce the high activation barrier usually associated with the cleavage of a C−C bond.[7] The reaction **2 → 3** may be described as an unusual oxidative coupling (metal goes from +3 to +4
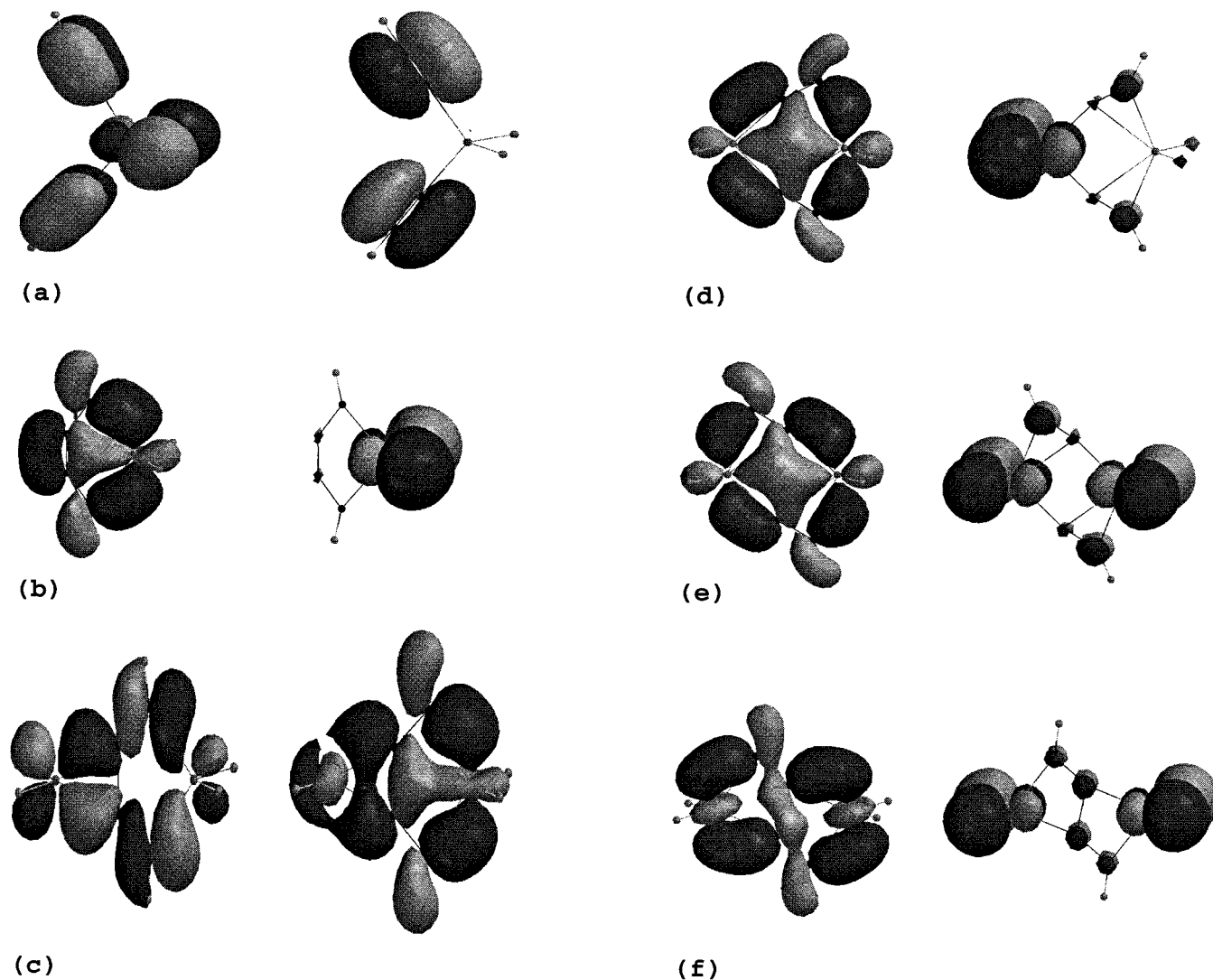
Figure 4. HOMO and HOMO-1 of various intermediates given in Scheme 4 for Zr complexes with L, R = H obtained at the B3LYP level using SPARTAN (ref 41).

oxidation state, with concomitant C−C coupling). Although it is tempting to conclude that Ti, being a first row transition metal, can accommodate both 16 and 18 electron counts, and Zr may not be able to do so, substituents may play a vital role as discussed above. The preference of the bisacetylide structure **2** for Ti with R = Si(CH$_3$)$_3$ suggests a complementary strategy to stabilize the C−C coupled structures for Zr. The preference for the C−C coupled product **3** might be increased with electron-withdrawing substituents such as fluorine. The selection of fluorine has an added advantage. Fluorine prefers an sp^3 carbon over an sp^2 carbon.[36] The preference for an sp^2 hybrid carbon over an sp hybrid carbon (eq 2)[37] is about 17 kcal/mol.

$$H-C\equiv C-F + H_2C=CH_2 \rightarrow H-C\equiv C-H +$$
$$H_2C=CHF \qquad \Delta H_f = -17 \text{ kcal/mol} \quad (2)$$
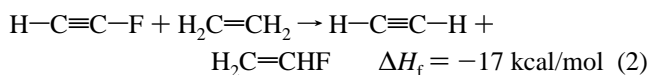
Accordingly the change in the thermodynamic preference on going from R = H to R = F (**8, 9 ca, cc, fa, fc**) is as expected.[38] The relative energy of 14.8 kcal/mol (13.5 kcal/mol at HF level) with R = H (**8fa, 9fa**) for Zr was brought down to −10.6 kcal/

(36) Giju, K. T.; Jemmis, E. D. *J. Mol. Struct. (THEOCHEM)* **1996**, *388*, 201−208.
(37) Smart, B. E. in *Molecular Structure and Energetics*; Liebman, J. F., Greenberg, A., Eds.; VCH: Weinheim, 1986; Vol. 3, p 141.
(38) Jemmis, E. D.; Giju, K. T. *Organometallics* **1997**, *16*, 1425.

mol with R = F (**8fc, 9fc**) at B3LYP level (−17.6 kcal/mol at HF level).[21] These trends will be of use in designing appropriate ligands so that even the Zr complex would lead to the C−C coupled products.

Further calculations for various acetylide substituents (R = H, F, CN) at the B3LYP/LANL2DZ level were carried out on simplified models **8** and **9** (**aa**, **ab**, **ac**, **da**, **db**, and **dc**) with C_{2h} symmetry. The relative energies indicate similar shifts between Ti and Zr complexes (Figure 7). The comparison of two sets of structures reveals that replacement of Cp by H has a larger effect on model Ti complexes (Figure 1). The Zr complexes are much less affected by such substitution. The transition structures (R = H) for conversion of **8** to **9** (**T89aa, ab, ac, da, ab, ac**) have been fully characterized, each with one imaginary frequency. The relative energies of the transition structures indicate that the C−C coupling is considerably more favorable for Ti than that of Zr (Figure 7).

Substitution of R = H by a cyanide CN group did not reverse the thermodynamic preference for M = Zr. Relative energy (9.1 kcal/mol) shows that coupled product is still less favored. Thus the cyanide group is not a sufficiently electron-accepting substituent to enforce shift in equilibrium on its own. Possibilities are that it may work in combination with various substituents on the Cp ligand. For M = Ti (**8ab and 9ab**) the

C–C Coupling and Cleavage Reactions

J. Am. Chem. Soc., Vol. 120, No. 28, 1998   6961

TiL$_2$ + H-CC-CC-H

65.8 (57.4) / 55.3 (49.5)

4+TiL$_2$

80.3 (67.6) / 74.0 (64.2)

14.5 (10.2) / 18.7 (14.7)

T69

103.2 (90.1) / 99.8 (87.9)

5+TiL$_2$

34.1 (31.9) / 34.5 (32.3)

44.4 (40.3) / 44.8 (42.5)

68.3 (57.8) / 65.6 (57.2)

6   T67

0.9 (0.5) / 1.7 (0.8)

21.3 (22.6) / 17.2 (16.8)

T78

12.0 (11.1) / 9.0 (7.9)

T89

1.7 (1.4) / 1.9 (1.1)

9

RE (kcal/mol)

13.4 (14.5) / 10.5 (10.0)

10.4 (11.7) / 8.6 (8.9)

7   8

Figure 5. Potential energy surface for the mechanism of C–C coupling reaction given in Scheme 6 involving Ti complexes. Reaction energies corrected for ZPE and the Gibbs free energy changes (in parentheses) are in kilocalories per mole. The upper numbers of the pair corresponds to L = H (**aa**) and the lower numbers to L = Cl (**ba**).

ZrL$_2$ + H-CC-CC-H

84.8 (77.3) / 88.1 (93.2)

4+ZrL$_2$

94.2 (82.2) / 100.2 (90.9)

9.4 (4.9) / 12.1 (7.7)

T69

5+ZrL$_2$

33.4 (31.7) / 34.6 (33.1)

44.5 (41.5) / 46.5 (43.3)

113.0 (98.5) / 122.9 (110.3)

76.4 (65.9) / 84.3 (76.0)

6   T67

0.3 (-0.3) / 0.1 (-0.1)

27.5 (27.4) / 26.6 (26.5)

T78

15.5 (14.4) / 15.5 (14.3)

T89   9

0.7 (0.1) / 0.7 (0.0)

RE (kcal/mol)

14.3 (13.8) / 13.6 (13.1)

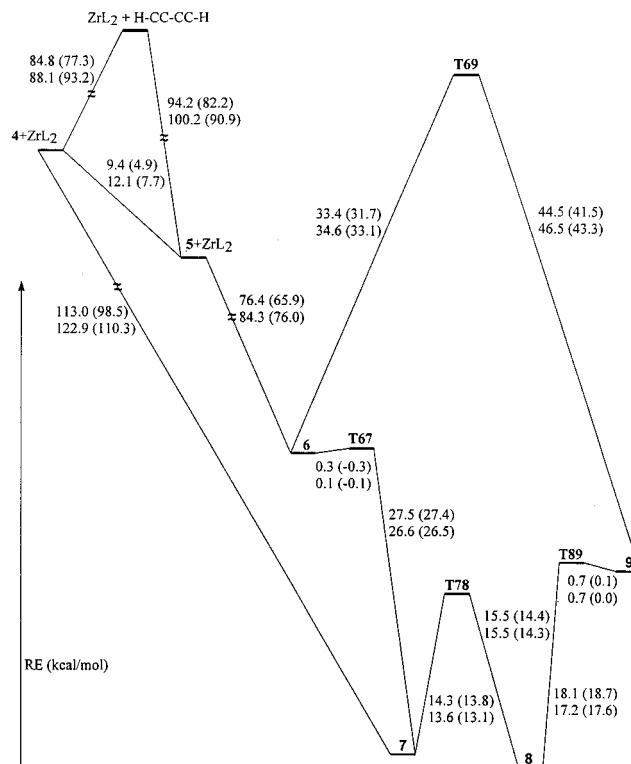18.1 (18.7) / 17.2 (17.6)

7   8

Figure 6. Potential energy surface for the mechanism of C–C coupling reaction given in Scheme 6 involving Zr complexes. Reaction energies corrected for ZPE and the Gibbs free energy changes (in parentheses) are in kilocalories per mole. The upper numbers of the pair corresponds to L = H (**aa**) and the lower numbers to L = Cl (**ba**).

reaction energy (0.5 kcal/mol) indicated a thermoneutral equilibrium. On the other hand for R = F both Ti and Zr complexes favor C–C coupled structures (Figure 7).

Qualitative molecular orbital calculations did not indicate appreciable differences between the Walsh diagrams for the process **8 → 9** for Ti and Zr complexes.[20] The differences in the ionic radii between Ti and Zr was suggested as another explanation. The larger size of Zr leads to longer Zr–acetylene distances which in turn leads to longer C3–C4 distance (3.003 Å) in **8fa**. In the isostructural Ti complex (**8ca**) the C3–C4 distance is reduced to 2.605 Å, which is further along the path of C–C bond formation. We find that fluorine substitution also helps in reducing the C3–C4 distance; it is calculated to be 2.985 Å in **8fc**. But these are comparatively longer distances and would it suffice as an explanation for the feasibility of a C–C bond formation? These arguments become even more meaningful in the comparison of barrier heights. During the process of C–C bond formation the C3–C4 distance (see Scheme 5 for numbering) goes from 2.786 Å → 1.964 Å → 1.607 Å (**8aa → T89aa → 9aa**) for Ti complexes (Table 2). A similar variation in Zr complexes is 2.986 Å → 1.944 Å → 1.637 Å (**8da → T89da → 9da**). This trend is seen in all **8 → 9** transformations. What are the other factors which may provide better understanding to the stability of **8fa** in relation to **9fa**?

There are some interesting features of the geometries of **8** vis-à-vis the relative energies of the models for **8** and **9**. We examined the possibility of the dependence of the relative thermodynamic stability of the coupled and the uncoupled complexes on the strength of the metal–metal interaction in **8**. For M = Ti, M–M distance 3.215 Å (**8aa**), 3.225 Å (**8ac**), and 3.191 Å (**8ab**) roughly followed the respective relative energy values 8.7 kcal/mol (**8aa → 9aa**), −9.1 kcal/mol (**8ac → 9ac**),

and 0.5 kcal/mol (**8ab → 9ab**). For M = Zr, M–M distance 3.469 Å (**da**), 3.509 Å (**8dc**), and 3.468 Å (**8db**) correlated respectively to the relative energy values 17.4 kcal mol^{-1} (**8da → 9da**), −3.9 kcal/mol (**8dc → 9dc**), and 8.6 kcal/mol (**8db → 9db**). However we feel that the changes in M–M distances is not large enough to attribute totally the substantial relative energy differences to the bond strength variations. Similarly in complexes with Cp ligands the M–M distances 3.614 Å (**8fa**) and 3.735 Å (**8fc**) correlated respectively to the relative energy values 14.8 kcal/mol (**8fa → 9fa**) and −10.6 kcal/mol (**8fc → 9fc**). Here the variation in M–M distance is significant. Thus it may be inferred that the isomerization reaction (**8 → 9**) becomes exothermic as the M–M distance is longer because **8** is less favorable with longer M–M distance. The nature of the substituent R on the acetylide affects the M–M distance. At a given M–M distance the Zr–Zr interaction may be stronger, making **8** more favorable. This is in tune with the general observation that within a group the M–M bond energies in the transition metal series increase with atomic number.[39] However these arguments are to be taken with caution because the bond energy for a regular Ti–Ti bond in Cl$_3$Ti–TiCl$_3$ is only ∼17 kcal/mol.[40] On the other hand C3–C4 distance in **8** does not show a similar dependence on relative energy. It is almost random. The M2–C3–C5 angles show variations depending on the substituents R. These angles are 164.9° (**8ac**), 166.2° (**8aa**), and 168.2° (**8ab**) when M = Ti. Similar changes are also observed for M = Zr with angles 166.2° (**8dc**), 167.9° (**8da**), and 169.8° (**8db**). This analysis shows that the maximum

(39) Kochi, J. K. *Organometallic Mechanisms and Catalysis*; Academic Press: New York, 1978; Chapter 11.

(40) Stahl, M.; Pidun, U.; Frenking, G. *Angew. Chem., Int. Ed. Engl.* **1997**, *36*, 2234.

(41) SPARTAN, Version 4.1, Wavefunction, Inc., Irvine, CA.

Table 1.   Important Geometric Parameters of the Structures **16−23** at the HF and B3LYP Levels[a]

molecule	M1−M2	M1−C3	M1−C4	M1−C5	M1−Cp	C3−C4	C3−C5	M1−C3−M2	C3−M1−C4	M2−C3−C5	C4−M1−C5
2c	3.550	2.394	2.056	2.312		2.706	1.253	106.0	74.0	176.0	105.0
2i	3.522	2.428	2.191	2.408		2.990	1.260	99.0	80.0	173.0	111.0
8ca	3.603	2.477	2.010	2.181	2.190	2.714	1.270	106.4	73.4	168.0	104.4
	3.694	*2.485*	*2.010*	*2.175*	*2.162*	*2.605*	*1.293*	*110.1*	*69.9*	*171.1*	*101.2*
9ca	4.155	2.400	2.044	2.038	2.167	1.615	1.333	138.3	41.7	163.6	75.4
	4.150	*2.361*	*2.071*	*2.050*	*2.147*	*1.584*	*1.348*	*138.8*	*41.4*	*161.3*	*75.9*
8fa	3.608	2.540	2.191	2.394	2.345	3.081	1.265	99.1	80.9	168.0	110.4
	3.614	*2.510*	*2.177*	*2.368*	*2.309*	*3.003*	*1.287*	*100.7*	*79.3*	*169.3*	*109.8*
9fa	4.461	2.544	2.201	2.199	2.339	1.654	1.349	140.0	40.0	160.2	72.0
	4.448	*2.513*	*2.214*	*2.192*	*2.301*	*1.628*	*1.362*	*140.4*	*39.6*	*159.1*	*72.4*
9cc	4.334	2.516	2.066	2.062	2.137	1.555	1.327	141.9	38.1	163.2	69.9
	4.230	*2.408*	*2.083*	*2.034*	*2.132*	*1.542*	*1.348*	*140.7*	*39.3*	*161.7*	*73.4*
8fc	3.899	2.658	2.176	2.285	2.327	2.898	1.289	107.1	72.9	166.3	101.9
	3.735	*2.595*	*2.168*	*2.295*	*2.300*	*2.985*	*1.299*	*103.0*	*77.0*	*165.1*	*107.1*
9fc	4.608	2.630	2.223	2.217	2.316	1.576	1.339	143.3	36.7	159.3	67.3
	4.529	*2.548*	*2.230*	*2.184*	*2.288*	*1.554*	*1.359*	*142.8*	*37.2*	*158.2*	*161.7*

[a] Experimental values of the related complexes are given for **2c** and **2i**. Values in *italics* are at the B3LYP level. The bond lengths in angstroms and the bond angles in degrees. The numbering is same as given in Scheme 5.
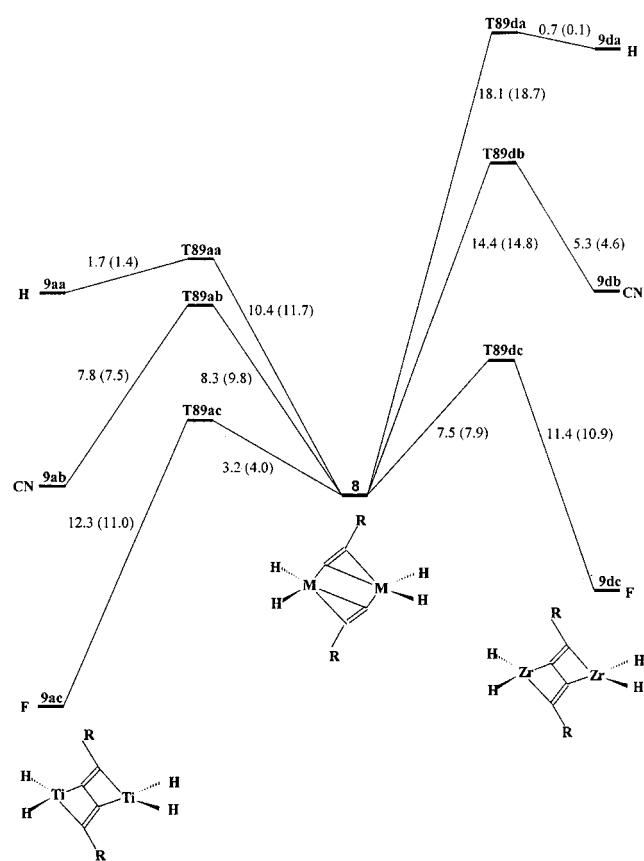
Figure 7. Potential energy diagram for the isomerization of **8** → **9** at the B3LYP level. Reaction energies corrected for ZPE and the Gibbs free energy changes (in parentheses) are in kilocalories per mole.

angle is for R = CN and minimum for R = F. Thus there is a stabilization due to the π-interaction of the acetylide group, −C≡C−R, which can also contribute to the stabilization of **8** though the order of relative energy is not followed directly. It is the CN group which will contribute more in this manner despite its considerable σ-electron withdrawal nature. MOs (Figure 4e,f) show the possible delocalization due to π-bonds.

(d) Natural Charge Analysis. Further understanding of the structure and bonding in these molecules is attempted from the charge analysis. Charges on metal and acetylide carbons are given in Table 3. Formally oxidation state +3 can be assigned to the metal in **8** which would make it a 17e complex with additional metal−metal interactions mediated through the bridg-

ing ligands. A formal oxidation state of +4 for the metal in **9** make it a 16e electron complex. Thus there should be approximately a +1 charge difference for the metal centers between complexes **8** and **9**. But the charges on metal centers calculated for these molecules indicate that there is no major charge difference on metals between **8** and **9** making the formal charge assignment insignificant as known for a number of molecules. The metals bear similar magnitude of charges which do not indicate the difference of a positive charge between two types of isomers, once again reminding us that oxidation state is what it is, a model.

Generally in all the type **8** structures, the metal has less positive charge than the type **9** complexes as expected from the formal oxidation state assignment. On the other hand acetylide carbon, C3, has less negative charge in **8** than **9**. Hence the comparison of **8** and **9** complexes demonstrates that the M−C3 bond is more ionic in the latter than in the former. For L = H, the Ti−C3 bond is less ionic than the Zr−C3 bond. For L = H and M = Ti or Zr, the charge on metal varies in the order for R = CN > H > F in **8**. In **9** this order changes a little as R = H > CN > F with the same metal. This change in the order may be a consequence of different hybridizations at C5 in the two types of complexes. The charges at C3 varies in the order R = F > H > CN in **8** and R = H > F > CN in **9** for L = H. At C5, it is R = H > CN > F in both **8** and **9**. Charge analysis is similar with L = Cl.

Extension of this analysis to complexes where ligand is cyclopentadienyl (**8,9 ca, fa, cc, fc**) provide a clearer view with regard to the nature of bonding in these realistic complexes. With L = Cp, M = Ti, and R = H, metal charge becomes significantly less positive and C3 becomes less negative, indicating the back-bonding available from Cp to the metal and consequent tendency toward more covalent bonding interaction compared to those in the simplified models. But such a reduction in charges is comparatively less for M = Zr compared to M = Ti. Zr holds larger positive charges in these complexes. On the other hand the charges on Cp give contrasting variations between Ti and Zr complexes. Total charge on Cp ligands are near zero in Ti complexes while it is near −0.3 in Zr complexes. Hence the interaction between the metal and Cp is more covalent in the former while it is more ionic in the latter. Substitution of H by F (**8fc**) has not diminished the magnitude of the positive charge on Zr significantly. Thus the charge analysis indicate that there is a major electrostatic contribution due to the metal−ligand interaction toward the possible antiferromagnetic interac-

Table 2.   Important Geometric Parameters of the Structures **8** and **9** and the Transition Structures at the B3LYP Level[a]

molecule	M1−M2	M1−C3	M1−C4	M1−C5	C3−C4	C3−C5	M1−C3−M2	C3−M1−C4	M2−C3−C5	C4−M1−C5
8aa	3.215	2.253	1.994	2.135	2.786	1.289	98.2	81.8	166.2	115.8
9aa	4.002	2.285	2.019	1.989	1.607	1.363	136.7	43.3	163.4	79.7
T89aa	3.872	2.345	1.982	2.012	1.964	1.337	126.8	53.2	174.3	87.9
8ab	3.191	2.233	1.994	2.170	2.783	1.291	97.8	82.2	168.2	116.2
9ab	4.054	2.311	2.024	2.009	1.560	1.406	138.5	41.5	161.7	77.7
T89ab	3.840	2.379	1.974	2.046	2.092	1.333	123.5	56.5	177.3	90.5
8ac	3.225	2.275	1.982	2.116	2.794	1.296	98.3	81.7	164.5	115.8
9ac	4.070	2.308	2.033	1.982	1.536	1.369	139.2	40.8	162.0	77.1
T89ac	3.775	2.438	1.964	2.039	2.313	1.327	117.7	62.3	174.5	95.3
8da	3.469	2.413	2.157	2.300	2.986	1.294	98.6	81.4	167.9	113.2
9da	4.364	2.478	2.174	2.156	1.637	1.372	139.4	59.7	160.3	74.1
T89da	4.255	2.519	2.144	2.170	1.944	1.350	131.5	48.5	169.0	80.8
8db	3.468	2.406	2.158	2.334	2.978	1.297	98.7	81.3	169.8	113.0
9db	4.438	2.513	2.184	2.181	1.574	1.380	141.6	38.4	158.3	71.6
T89db	4.232	2.563	2.137	2.204	2.089	1.345	128.2	51.8	172.5	83.5
8dc	3.509	2.452	2.147	2.282	2.989	1.301	99.2	80.8	166.2	112.4
9dc	4.441	2.508	2.187	2.156	1.558	1.373	142.0	38.0	158.8	71.1
T89dc	4.185	2.622	2.127	2.195	2.299	1.337	123.3	56.7	180.0	87.4

[a] The bond lengths in Å and the bond angles in degree. The numbering is same as given in Scheme 5.

Table 3.   Natural Charges on Atoms and Wiberg Bond Indices in the Structures **8** and **9** and the Transition Structures at the B3LYP Level

molecule	M1	C3	C5	R7	L	M1−M2	M1−C3	M1−C4	M1−C5	C3−C4	C3−C5
8ca	0.286	−0.103	−0.382	0.238	−0.019	0.324	0.226	0.938	0.604	0.144	2.200
9ca	0.392	−0.187	−0.322	0.220	−0.052	0.262	0.252	0.710	0.842	0.876	1.811
8fa	1.127	−0.372	−0.441	0.238	−0.276	0.255	0.307	0.831	0.502	0.084	2.287
9fa	1.335	−0.401	−0.516	0.218	−0.318	0.169	0.238	0.653	0.774	0.889	1.813
9cc	0.364	−0.255	0.276	−0.384	−0.001	0.205	0.249	0.686	0.834	0.937	1.711
8fc	1.123	−0.410	0.138	−0.360	−0.245	0.186	0.293	0.853	0.560	0.134	2.127
9fc	1.323	−0.455	0.086	−0.388	−0.283	0.143	0.229	0.618	0.762	0.979	1.722
8aa	0.888	−0.362	−0.353	0.258	−0.215	0.316	0.366	0.892	0.556	0.105	2.270
9aa	1.384	−0.496	−0.485	0.239	−0.321	0.133	0.250	0.665	0.853	0.926	1.820
T89aa	0.984	−0.354	−0.437	0.251	−0.223	0.192	0.273	0.850	0.812	0.582	1.962
8ab	0.899	−0.294	−0.255	0.268	−0.185	0.296	0.375	0.879	0.462	0.102	2.126
9ab	1.049	−0.316	−0.345	0.283	−0.196	0.197	0.253	0.720	0.774	1.014	1.662
T89ab	1.012	−0.272	−0.372	0.284	−0.189	0.180	0.245	0.879	0.677	0.508	1.882
8ac	0.854	−0.427	0.258	−0.296	−0.195	0.204	0.390	0.909	0.561	0.124	2.138
9ac	0.987	−0.428	0.179	−0.330	−0.203	0.196	0.282	0.708	0.871	1.046	1.665
T89ac	0.946	−0.380	0.150	−0.321	−0.198	0.170	0.254	0.935	0.733	0.402	1.943
8da	1.392	−0.522	−0.432	0.253	−0.346	0.261	0.358	0.830	0.524	0.108	2.277
9da	1.522	−0.495	−0.530	0.233	−0.365	0.171	0.235	0.677	0.803	0.941	1.830
T89da	1.518	−0.361	−0.487	0.243	−0.361	0.146	0.230	0.760	0.755	0.662	1.957
8db	1.419	−0.450	−0.332	0.263	−0.320	0.238	0.356	0.816	0.430	0.110	2.128
9db	1.590	−0.429	−0.458	0.279	−0.340	0.152	0.199	0.656	0.685	1.034	1.683
T89db	1.560	−0.406	−0.476	0.282	−0.332	0.128	0.213	0.783	0.619	0.582	1.876
8dc	1.382	−0.582	0.168	−0.306	−0.331	0.211	0.363	0.839	0.528	0.131	2.157
9dc	1.529	−0.543	0.056	−0.347	−0.347	0.151	0.225	0.650	0.778	1.044	1.713
T89dc	1.496	−0.515	0.036	−0.336	−0.341	0.120	0.221	0.830	0.685	0.484	1.938

tion mediated through the bridging acetylides leading to the shortening of Zr−Zr distance compared to Ti−Ti distance in **8**.

Conclusions

Reaction mechanisms investigated in this paper suggest that C−C coupled steps for **6** → **9** via **T69** are energetically very high, and there exists pathways with lower barriers such as **6** → **T67** → **7** → **T78** → **8** → **T89** → **9**. The important step which differentiates Ti and Zr in the mechanism is the dynamic isomerization reaction of **8** → **9**. The unusual C−C coupling observed in dimeric bis(η^5-cyclopentadienyl)phenylethynyltitanium complex and the lack of it in the corresponding zirconium complex are consequences of the thermodynamic energy differences. Highly electron withdrawing substituents on the ethynyl bridging group might help in getting structure **9fa** to be competitive to **8fa**. In general, the model studies indicate that Ti is preferred over Zr for the C−C coupled product **9** when R = H and CN. When R = F, the C−C coupled structures (**9**)

are preferred for both Ti and Zr over the uncoupled structures (**8**). By using appropriate substituents on the bridging ethynyl ligand, it should be experimentally possible to obtain the C−C coupled product even with Zr. While the ionic interaction of Cp ligand with metal center is attributed for the unusually shorter Zr−Zr distance in **8**, we feel that this may not be responsible for the shifts in thermodynamic equilibrium. The uniformly higher barrier calculated for the C−C coupling of the Zr complexes is in tune with the longer distance to be traversed by the carbons in reaching the transition structure.

Supporting Information Available: Total energy, zero point energy, thermal correction to Gibbs free energy, number of imaginary frequencies, lowest frequency value, and Cartesian coordinates are given for all the structures (33 pages, print/

PDF). See any current masthead page for ordering information and Web access instructions.

JA972710J